

# Nonlinear optical detection of a ferromagnetic state at the single interface of an antiferromagnetic $\text{LaMnO}_3/\text{SrMnO}_3$ double layer

Naoki Ogawa\*

Research Center for Advanced Science and Technology (RCAST), The University of Tokyo,  
Komaba, Meguro-ku, Tokyo 153-8904, Japan

Takuya Satoh

Institute of Industrial Science (IIS), The University of Tokyo, Komaba, Meguro-ku, Tokyo 153-8904, Japan

Yasushi Ogimoto<sup>†</sup> and Kenjiro Miyano

Research Center for Advanced Science and Technology (RCAST), The University of Tokyo, Komaba, Meguro-ku, Tokyo 153-8904, Japan  
and CREST, Japan Science and Technology Agency, 4-1-8 Honcho, Kawaguchi, Saitama 332-0012, Japan

(Received 8 November 2008; published 23 December 2008)

Emergence of a ferromagnetic state at the single interface of two antiferromagnetic perovskite manganites,  $\text{LaMnO}_3$  and  $\text{SrMnO}_3$ , has been detected with nonlinear magneto-optical Kerr rotation. The samples are composed of approximately four unit cells of each material, with reversed stacking sequence. The existence and orientations of the interface dipole or that of so-called toroidal moment were determined through phase-sensitive second-harmonic detection. Characterization of multiferroic states at the single interfaces, and non-negligible effect of surfaces on the Kerr rotation are demonstrated.

DOI: [10.1103/PhysRevB.78.212409](https://doi.org/10.1103/PhysRevB.78.212409)

PACS number(s): 75.70.Cn, 78.20.Ls, 42.65.Ky

Surfaces and interfaces have physical properties distinct from those of bulk due to their broken symmetries. Engineering and/or spontaneous emergence of unique material properties at interfaces of perovskite oxides became considerably important in modern electronics. Atomically sharp interfaces of these oxides can be readily fabricated by state-of-the-art thin-film growth techniques. In these artificial materials, electronic (orbital), magnetic, and atomic reconstructions with a scale of single atomic layer are driven by charge transfer, exchange interactions, and strain effects, leading to exotic electronic states bound to the interface. Recent examples are highly conducting and superconducting layers between insulating oxides  $\text{LaAlO}_3/\text{SrTiO}_3$  (Refs. 1 and 2) and emergence of ferromagnetism at the interface of antiferromagnetic (AF) insulators  $\text{LaMnO}_3/\text{SrMnO}_3$  (Ref. 3) or at the interface of AF insulator  $\text{CaMnO}_3$  and paramagnetic metal  $\text{CaRuO}_3$ .<sup>4</sup> Besides, magnetism at the interfaces has another important aspect as an essential ingredient to achieve functional multiferroic properties.<sup>5</sup>

Optical second-harmonic generation (SHG) is a versatile and nondestructive probe to study buried interfaces.<sup>6</sup> Usually, magnetization alone does not break the space-inversion symmetry. However it can lower the symmetry of the interface, leading to the modification of the nonlinear susceptibility tensor.<sup>7</sup> For example, magnetization-induced second-harmonic generation (MSHG) has been utilized to study surface and interface magnetism.<sup>8,9</sup> In addition to the interface sensitivity, MSHG shows large nonlinear Kerr rotation,<sup>10,11</sup> whose origin has been ascribed to the simultaneous breaking of inversion (at interface) and time-reversal (by magnetization) symmetries. Recently, SHG is also successfully applied for detecting toroidal moments in multiferroic materials,<sup>12,13</sup> proving its high sensitivity to electronic and magnetic symmetries.

There have been several reports on the detection of elec-

tronic reconstructions at the interface of manganese oxides through linear<sup>14,15</sup> and nonlinear<sup>13,16</sup> optics. To enhance signal intensity, however, “tricolor” superlattices have been employed in most of the cases. The unavoidable presence of the two additional interfaces in these samples, whose effects cannot be separately measured, makes unambiguous interpretation difficult. A simpler characterization of a single isolated interface has been awaited.

In this Brief Report, we demonstrate the detection of ferromagnetism or breaking of time-reversal symmetry at the single interfaces of AF insulators  $\text{LaMnO}_3$  (LMO) and  $\text{SrMnO}_3$  (SMO) by means of nonlinear magneto-optical Kerr effect (NMOKE). These compounds are the end materials of a prototypical strongly correlated electron system,  $\text{La}_{1-x}\text{Sr}_x\text{MnO}_3$  (LSMO).<sup>17,18</sup> Here LMO has one  $e_g$  electron per Mn site ( $d^4$ ), which is expected to form alternating alignment of  $d_{3x^2-r^2}$  and  $d_{3y^2-r^2}$  orbitals, while SMO has no  $e_g$  electron ( $d^3$ ). In terms of magnetism, LMO and SMO are *A*-type and *G*-type AF insulators, respectively. At these heterointerfaces, charge transfer, due to the difference in the chemical potential, is correlated with the spin and orbital degrees of freedom, resulting in the formation of two-dimensional ferromagnetic layers as have been reported by many groups.<sup>3,14,19–23</sup> Since space-inversion and time-reversal symmetries are broken simultaneously, we have additional second-harmonic (SH) components induced by toroidal moment.<sup>12,24</sup> We also show that the direction of charge transfer or the orientations of the interface dipole and toroidal moments can be inferred from the measurements of relative phase of the nonlinear susceptibilities.

We prepared two samples having the same heterointerfaces,<sup>25</sup> with reversed stacking sequence, LMO on SMO and SMO on LMO, on  $(\text{LaAlO}_3)_{0.3}(\text{SrAl}_{0.5}\text{Ta}_{0.5}\text{O}_3)_{0.7}$  (LSAT)(001) substrates by pulsed laser deposition (for details, see Ref. 26). Both materials are approximately four unit

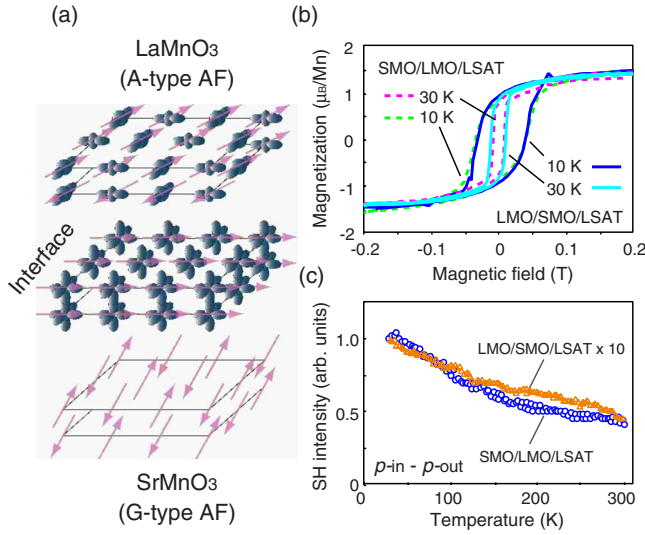


FIG. 1. (Color online) (a) A schematic of spin and orbital configurations at the interface of antiferromagnetic LaMnO<sub>3</sub> and SrMnO<sub>3</sub>. At the heterointerface, a ferromagnetic state is expected. (b) In-plane  $M$ - $H$  loops for the fabricated LMO/SMO and SMO/LMO interfaces at 10 and 30 K. (c) Temperature dependence of the SH intensity for  $p_{\text{in}}-p_{\text{out}}$  geometry. The data from LMO/SMO are multiplied by 10.

cells ( $\sim 1.6$  nm) in thickness, as controlled by monitoring the intensity oscillation of reflection high-energy electron diffraction (RHEED). These samples were mounted in an ultrahigh vacuum (UHV) cryostat, and SHG was measured with 800 nm fundamental light (150 fs duration at 1 kHz repetition rate) incident through a  $\lambda/2$  plate with  $90^\circ$  reflection geometry. The generated SH was directed to a glan prism, color filters, and a monochromator and detected with a photomultiplier tube. The SH signal was normalized by that of a reference KDP crystal and accumulated more than  $10^4$  times at each polarization configuration. The magnetic field was applied in plane ( $[100]$ ) of the samples with permanent magnets (up to  $\sim 0.1$  T [Fig. 2(a)]).

The spin and orbital reconstructions at the interface of LMO and SMO are illustrated in Fig. 1(a).<sup>14</sup> At the heterointerface, orbital-liquid and ferromagnetic spin alignment are expected. In fact, both fabricated samples undergo ferromagnetic transition at  $\sim 150$  K and show clear and almost identical hysteresis in  $M$ - $H$  curves at low temperature [Fig. 1(b)], indicating that both samples have flat interfaces with identical structure except for the stacking sequence.<sup>27</sup> The transition temperature and magnetic moment ( $\sim 1.5\mu_B/\text{Mn}$  site at low temperature) are consistent with those of previous reports on superlattice samples.<sup>14</sup>

At the heterointerface of cubic perovskites,  $4mm$  symmetry is expected, which has three independent components ( $\chi_{xx}^d = \chi_{yy}^d$ ,  $\chi_{zz}^d = \chi_{yy}^d$ , and  $\chi_{zz}^d$ ) in nonlinear optical susceptibility tensor  $\chi^{(2)}$ . In our setup, the SH signal is dominated by the interface dipole, which yields mainly  $p$ -polarized light. For  $p$ -polarization incidence and  $p$ -polarization reflection geometry ( $p_{\text{in}}-p_{\text{out}}$ ), SMO/LMO has about ten times larger SH intensity than LMO/SMO, but both samples show similar temperature dependence [Fig. 1(c)]. We performed polarization analysis<sup>28</sup> by assuming the refractive index of the non-

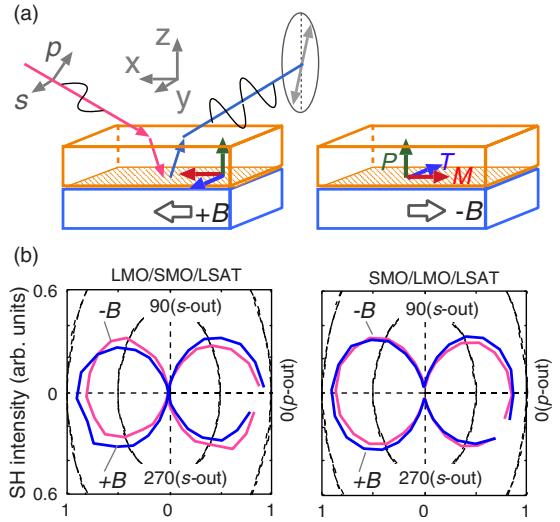


FIG. 2. (Color online) (a) Experimental geometry and coordination for the NMOKE measurement.  $s$ -polarized fundamental light incidents on the sample and polarization of the output SH is analyzed. The expected interface dipole ( $\mathbf{P}$ ), magnetic ( $\mathbf{M}$ ), and toroidal ( $\mathbf{T}$ ) moments are shown by arrows. (b) Detected polarization rotation for LMO/SMO and SMO/LMO samples at 30 K under the in-plane magnetic field of 0.1 T (indicated with  $\pm B$ ). By reversing the external magnetic field, the direction of polarization rotation changes.

linear layer to be that of an LSMO film.<sup>29</sup> We confirmed  $4mm$  symmetry at both interfaces, as expected, and found that  $\chi_{zzz}$  are more than 1 order of magnitude larger than other elements, indicating the formation of relatively large interface dipoles ( $\mathbf{P}$ ). This is consistent with the previous report on the same sample systems investigated with the Maker fringe technique.<sup>26</sup>

Figure 2(a) shows the optical setup for the NMOKE measurement. The samples were illuminated with  $s$ -polarized fundamental light, and the polarization of the reflected SH signal was analyzed. With the presence of magnetic moment ( $\mathbf{M}$ ) at the interface, now we have toroidal moment ( $\mathbf{T} = \mathbf{P} \times \mathbf{M}$ ) acting on the electrons as vector potential,<sup>17</sup> which induces  $s$ -polarized SH ( $\chi_{yyy}^m$ ). As a result, the polarization of the output SH will rotate (angle  $\phi$ ) depending on the direction of magnetic (or toroidal) moment, according to

$$\tan \phi \sim \text{Re} \frac{\beta \chi_{yyy}^m}{\alpha (\chi_{yy}^d + \chi_{zy}^m)}, \quad (1)$$

where  $\alpha$  and  $\beta$  are Fresnel factors and  $\chi_{zy}^d$ ,  $\chi_{yyy}^m$ , and  $\chi_{zy}^m$  are the elements of second-order nonlinear susceptibility induced by electric dipole ( $d$ ) and magnetic ( $m$ ) moments. Here the SH rotation induced by  $\chi_{yyy}^m$  is directly related to the toroidal moment, and the contribution from  $\chi_{zy}^m$  is in general negligible compared to  $\chi_{zy}^d$ .

Figure 2(b) shows the NMOKE measured at 30 K under in-plane magnetic field of 0.1 T. By reversing the direction of external magnetic field, we can clearly observe the change in the direction of rotation in the SH polarization. The rotation angle is larger for LMO/SMO, whose origin will be given later.

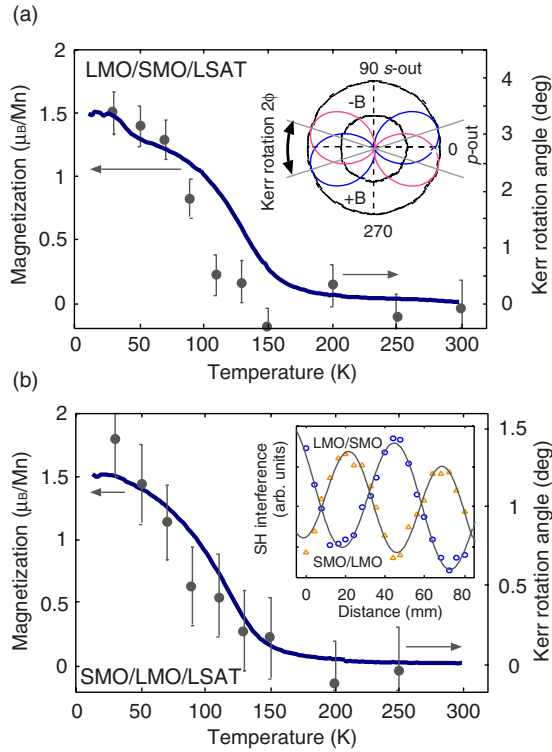


FIG. 3. (Color online) Temperature dependence of the Kerr rotation angle (filled circles with error bars) and magnetization (solid lines) for (a) LMO/SMO and (b) SMO/LMO, respectively. The magnetization was measured with a field cooling run under a magnetic field of 0.1 T. Inset in (a) shows a schematic of the Kerr rotations under opposite external magnetic fields. Inset in (b) shows the result of SH phase measurements, indicating that the generated SH signals from LMO/SMO and SMO/LMO are in the opposite phase ( $\sim\pi$  different). The solid lines are fits to Eq. (2).

Temperature dependence of the Kerr rotation angle, together with the magnetization, is shown in Fig. 3. For both samples, the rotation angles, which are proportional to the amplitude of the toroidal moment, closely follow the evolutions of the magnetization measured separately with a superconducting quantum interference device. We emphasize that these signals are from the single interfaces in  $\sim 3.2$ -nm-thick samples, which prove high sensitivity of the nonlinear optical method. We also fabricated single SMO and LMO films on LSAT substrates as control samples, and confirmed that the single SMO film does not have spontaneous magnetization. Single LMO film shows weak magnetic moment at low temperature<sup>3</sup> but does not show Kerr rotation within a current resolution.

To depict a clear picture on the multiferroic alignment of the moments, we performed the phase-sensitive SHG measurements<sup>30</sup> and determined the relative orientation of the dipole moments of both samples. For this measurement the samples were placed in the ambient air. A reference  $\alpha$ -quartz crystal was placed after the sample and displaced (distance  $d$ ) along the optical path to have a path-length-dependent interference of SH fields from the sample and the reference crystal; the latter is generated with the reflected fundamental light on the sample surface. Due to the disper-

sion of air, we have cosinelike interferogram after the SH interference,<sup>31</sup>

$$I_{2\omega}(d) = I_{2\omega}^0 + I_{2\omega}^1(d)\cos(4\pi\Delta n d/\lambda + \phi_0), \quad (2)$$

where  $\Delta n$  is the dispersion of the air,  $\lambda$  is the fundamental wavelength, and  $\phi_0$  is the initial phase difference. In our setup,  $2\pi$  phase shift corresponds to  $d \sim 50$  nm.<sup>32</sup> We include slight misalignment of the optical path in the interference amplitude  $I_{2\omega}^1(d)$ .

As shown in the inset of Fig. 3(b), the relative phases for LMO/SMO and SMO/LMO are nearly  $\pi$  different, indicating that the interface dipole moments are pointing in the opposite directions. This result also shows that the interface dipoles are well established, and the fabricated samples are not like a solid solution, which is consistent with the previous reports in that the charge transfer between LMO and SMO is expected to extend two to three unit cells from the interface.<sup>20,22</sup> Now we have a complete picture of the orientations of dipole, magnetic, and toroidal moments. For example, the upper side should correspond to LMO in the schematic of Fig. 2(a).

In Fig. 2(b), the SH polarization rotates in the same direction under the reversal of magnetic field for both samples, irrespective of the orientation of interface dipoles. This is because of the parities of the tensor elements<sup>7</sup> in Eq. (1), where  $\chi_{yyy}^m$  ( $\chi_{zyy}^{d,m}$ ) is odd (even) function of time-reversal operation. Therefore, for the reversal of the magnetic moment, only  $\chi_{yyy}^m$  changes its sign, which appears as the change in the direction of Kerr rotation. However, all the elements in Eq. (1) are odd function for space inversion; under the reversal of dipole moment, the overall sign, i.e., the direction of Kerr rotation, is left unaffected. Thus we have to measure the orientation of the dipole moments separately, as has been done in the above, to determine the multiferroic alignments of the respective moments.

In Figs. 3(a) and 3(b), the Kerr rotation angles differ by a factor of 2.4, although both interfaces have similar magnetization at low temperature ( $\sim 1.5\mu_B/\text{Mn}$  site). This is also related to Eq. (1), which shows that the rotation angle depends not only on  $\chi_{yyy}^m$  but also on the intensity of the  $p$ -polarized SH. In the real situation, the  $p$ -polarized SH has contributions from interfaces of LMO and SMO and also from the surfaces, where the space-inversion symmetry is broken. As shown in Fig. 1(c), SMO/LMO has approximately ten times larger  $p$ -polarized SH intensity, which has been explained with constructive (for SMO/LMO) and destructive (LMO/SMO) interferences of SH fields from the heterointerfaces and surfaces<sup>26</sup> (here the signals from film/substrate interfaces are negligible). After polarization analysis, we found approximately five times larger apparent  $\chi_{zyy}^d$  for SMO/LMO than LMO/SMO, which should result in five times smaller Kerr rotation for SMO/LMO. Although the expected difference in the rotation angle is larger than that of our observation, the apparent magnitude of the susceptibility tensor elements sensitively depends on the complex refractive index of the nonlinear layer (i.e., Fresnel factors),<sup>28</sup> which may differ from our assumption. This result indicates the possibility of increasing Kerr rotation angle by modifying the surface while film preparation.

We note in passing that  $\chi_{yyy}^m$  is imaginary by symmetry consideration.<sup>7</sup> The Kerr rotation, therefore, vanishes if all the Fresnel factors and  $\chi_{zy}^d$  are real in Eq. (1): some of them must be complex. In the present experiment, the fundamental wavelength is above the optical gap of both LMO and SMO thin films, thus, providing phase shift in the optical response. Although we do not know the absolute phases of  $\chi_{xz}^d$ ,  $\chi_{zx}^d$ , and  $\chi_{zz}^d$  at this moment, it is important to choose the fundamental wavelength suitable for the sample system to utilize the complex optical response to have larger Kerr rotation. It has been pointed out that the incident angle of the fundamental light is also essential for the optimal Kerr rotation.<sup>16</sup>

In summary, we have detected the multiferroic state, resulting from the electronic and magnetic reconstructions at

the single interfaces of LaMnO<sub>3</sub> and SrMnO<sub>3</sub> thin films through NMOKE and phase-sensitive SH techniques. We demonstrated that we have the sensitivity of magnetic moment down to single interfaces within the  $\sim 3.2$ -nm-thick samples, with the complete assignment of the orientations of dipole, magnetic, and toroidal moments. The large interface dipole enhances the magnetic contribution to the nonlinear susceptibility, enabling us to observe sufficient Kerr rotation.

We are grateful to H. Tamaru for technical assistance. This work has been supported by JSPS KAKENHI (Grant No. 19840014) and MEXT TOKUTEI (Grant No. 16076207).

\*ogawa@myn.rcast.u-tokyo.ac.jp

<sup>†</sup>Also at Fuji Elec. Adv. Tech., Hino, Tokyo 191-8502, Japan.

- <sup>1</sup>A. Ohtomo and H. Y. Hwang, *Nature (London)* **427**, 423 (2004).
- <sup>2</sup>N. Reyren, S. Thiel, A. D. Caviglia, L. F. Kourkoutis, G. Hammerl, C. Richter, C. W. Schneider, T. Kopp, A.-S. Rüetschi, D. Jaccard, M. Gabay, D. A. Muller, J.-M. Triscone, and J. Mannhart, *Science* **317**, 1196 (2007).
- <sup>3</sup>T. Koida, M. Lippmaa, T. Fukumura, K. Itaka, Y. Matsumoto, M. Kawasaki, and H. Koinuma, *Phys. Rev. B* **66**, 144418 (2002).
- <sup>4</sup>K. S. Takahashi, M. Kawasaki, and Y. Tokura, *Appl. Phys. Lett.* **79**, 1324 (2001).
- <sup>5</sup>Y. Tokura, *J. Magn. Magn. Mater.* **310**, 1145 (2007).
- <sup>6</sup>Y. R. Shen, *The Principles of Nonlinear Optics* (Wiley, New York, 1984).
- <sup>7</sup>R.-P. Pan, H. D. Wei, and Y. R. Shen, *Phys. Rev. B* **39**, 1229 (1989).
- <sup>8</sup>W. Hübner and K. H. Bennemann, *Phys. Rev. B* **40**, 5973 (1989).
- <sup>9</sup>A. Kirilyuk and T. Rasing, *J. Opt. Soc. Am. B* **22**, 148 (2005).
- <sup>10</sup>B. Koopmans, M. G. Koerkamp, T. Rasing, and H. van den Berg, *Phys. Rev. Lett.* **74**, 3692 (1995).
- <sup>11</sup>Y. Ogawa, Y. Kaneko, J. P. He, X. Z. Yu, T. Arima, and Y. Tokura, *Phys. Rev. Lett.* **92**, 047401 (2004).
- <sup>12</sup>B. B. van Aken, J.-P. Rivera, H. Schmid, and M. Fiebig, *Nature (London)* **449**, 702 (2007).
- <sup>13</sup>H. Yamada, Y. Ogawa, Y. Ishii, H. Sato, M. Kawasaki, H. Akoh, and Y. Tokura, *Science* **305**, 646 (2004).
- <sup>14</sup>N. Kida, H. Yamada, H. Sato, T. Arima, M. Kawasaki, H. Akoh, and Y. Tokura, *Phys. Rev. Lett.* **99**, 197404 (2007).
- <sup>15</sup>H. B. Zhao, K. J. Smith, Y. Fan, G. Lüpke, A. Bhattacharya, S. D. Bader, M. Warusawithana, X. Zhai, and J. N. Eckstein, *Phys. Rev. Lett.* **100**, 117208 (2008).
- <sup>16</sup>Y. Ogawa, H. Yamada, T. Ogasawara, T. Arima, H. Okamoto, M. Kawasaki, and Y. Tokura, *Phys. Rev. Lett.* **90**, 217403 (2003).
- <sup>17</sup>For a review, Y. Tokura, *Rep. Prog. Phys.* **69**, 797 (2006).
- <sup>18</sup>J. Hemberger, A. Krimmel, T. Kurz, H.-A. Krug von Nidda, V. Yu. Ivanov, A. A. Mukhin, A. M. Balbashov, and A. Loidl, *Phys. Rev. B* **66**, 094410 (2002).
- <sup>19</sup>Ş. Smadici, P. Abbamonte, A. Bhattacharya, X. Zhai, B. Jiang, A. Rusydi, J. N. Eckstein, S. D. Bader, and J.-M. Zuo, *Phys. Rev. Lett.* **99**, 196404 (2007).
- <sup>20</sup>H. Yamada, M. Kawasaki, T. Lottermoser, T. Arima, and Y. Tokura, *Appl. Phys. Lett.* **89**, 052506 (2006).
- <sup>21</sup>A. Bhattacharya, X. Zhai, M. Warusawithana, N. Eckstein, and S. D. Bader, *Appl. Phys. Lett.* **90**, 222503 (2007).
- <sup>22</sup>C. Adamo, X. Ke, P. Schiffer, A. Soukiassian, M. Warusawithana, L. Maritato, and D. G. Schlom, *Appl. Phys. Lett.* **92**, 112508 (2008).
- <sup>23</sup>B. R. K. Nanda and S. Satpathy, *Phys. Rev. B* **78**, 054427 (2008).
- <sup>24</sup>H. J. Ross, B. S. Sherborne, and G. E. Stedman, *J. Phys. B* **22**, 459 (1989).
- <sup>25</sup>We note that, strictly speaking, the interfaces are LaO/MnO<sub>2</sub> and SrO/MnO<sub>2</sub> for LMO/SMO and SMO/LMO samples, respectively. However, this difference did not affect our observations probably because of the extent of the charge transfer. In fact, *M-H* and *M-T* properties of these two samples are almost the same as shown in Figs. 1(b) and 3.
- <sup>26</sup>T. Satoh, K. Miyano, Y. Ogimoto, H. Tamaru, and S. Ishihara, *Phys. Rev. B* **72**, 224403 (2005).
- <sup>27</sup>S. J. May, A. B. Shah, S. G. E. te Velthuis, M. R. Fitzsimmons, J. M. Zuo, X. Zhai, J. N. Eckstein, S. D. Bader, and A. Bhattacharya, *Phys. Rev. B* **77**, 174409 (2008).
- <sup>28</sup>We followed N. Bloembergen and P. S. Pershan, *Phys. Rev.* **128**, 606 (1962).
- <sup>29</sup>J. Mistrík, T. Yamaguchi, M. Veis, E. Liskova, S. Visnovsky, M. Koubaa, A. M. Haghiri-Gosnet, Ph. Lecoeur, J. P. Renard, W. Prellier, and B. Mercey, *J. Appl. Phys.* **99**, 08Q317 (2006).
- <sup>30</sup>K. Kemnitz, K. Bhattacharyya, J. M. Hicks, G. R. Pinto, K. B. Eisenthal, and T. F. Heinz, *Chem. Phys. Lett.* **131**, 285 (1986).
- <sup>31</sup>R. Stolle, K. J. Veenstra, F. Manders, Th. Rasing, H. van den Berg, and N. Persat, *Phys. Rev. B* **55**, R4925 (1997).
- <sup>32</sup>A. L. Mifflin, M. J. Musorrafiti, C. T. Konek, and F. M. Geiger, *J. Phys. Chem. B* **109**, 24386 (2005).